

CHEMICAL DURABILITY AND THERMAL STABILITY OF Er³⁺-DOPED ZINC TELLURITE GLASS CONTAINING SILVER NANOPARTICLES

M. REZA DOUSTI^{a,b,*}, PAYMAN GHASSEMI^c, M.R. SAHAR^a, ZAHRA ASHUR MAHRAZ^a

^a*Advanced Optical Material Research Group, Department of Physics, Faculty of Science, Universiti Teknologi Malaysia, Skudai, 81310 Johor, Malaysia*

^b*Department of Physics, Tehran-North Branch, Islamic Azad University, Tehran, Iran*

^c*Faculty of Chemical Engineering, Universiti Teknologi Malaysia, Skudai, 81310 Johor, Malaysia*

Improving the chemical durability and thermal stability of rare-earth doped glasses is a challenging issue. Glasses with composition (80-x)TeO₂-20ZnO-1Er₂O₃-xAgCl (x=0, 0.5, 1, 2 and 3 mol%) were prepared by melt quenching method. The chemical durability and water resistivity of those glasses are investigated by measuring the weight of samples after and before weathering by water and ammonium hydroxide. Variation of surface morphology is observed by AFM, SEM and EDX techniques. The weight loss is explained in terms of dissolution of glass in the immersed solution. Increments in the weight of samples are attributed to clustering and deposition of elements on the glass surface. The weight loss over twenty one days showed that addition of AgCl decreases the resistivity against water and ammonium solution. The introduction of AgCl found to increase the thermal stability and resulted in stronger glass networks. Also, the fragility is improved by incorporation of AgCl as revealed by the broadening of glass transition width. Our observation may be useful for the fabrication of nanophotonic devices in different environments.

(Received December 20, 2013; Accepted March 3, 2014)

Keywords: Chemical durability, Thermal stability, Tellurite glass, Silver nanoparticles

1. Introduction

Tellurite glass shows significant optical properties such as large linear and nonlinear refractive index, wide transparency window and low phonon cut-off energy. Their physical properties, e.g. high density values, also make them worthy to apply in different optical applications. Thermal stability, chemical durability and rare earth (RE) solubility of tellurite glasses are also other important characteristics which nominate them as excellent candidates for wide range of applications more appropriate than silicate, phosphate and borate based glasses. Large thermal stability of tellurite glasses make them as a good solid state material doped with RE ions, which work even at high temperature ranges. Recently, in order to achieve strong luminescence emissions of RE-doped heavy metal oxide (HMO) glasses, noble metallic nanoparticle (NP) were introduced by different authors [1-3] and except few reports on quench [4,5] typically the results met the enhancements in optical properties.

The chemical durability of oxide glasses are usually studied by investigating the chemical reaction by water, alkali or acid solution to surface of glass samples. The surface scratches and roughness of the glass are also important factors to achieve stronger glasses. Therefore, well-polished glasses are more stable than rugged surfaces in the presence of etching and reducing

* Corresponding author: mrdphysics@gmail.com

agents. Corrosion of glasses usually takes place by three lines of attack. First, an ion exchange reaction leads to dissolution of one or more components of glass and leaving a spongy layer on the surface. This “leaching” attack defects the surface by tarnishing or staining. The second mechanism is “etching”, where glass structure dissolves totally. Finally, “shiroyake” processes in which the insoluble elements deposit on the surface of glass [6].

Zinc tellurite glass is one of the most studied glasses and their structural, thermal [7-9], and optical [10] properties were reported far and wide. Stavrou et al. [7] demonstrated that $(100-x)\text{TeO}_2-x\text{ZnO}$ glassy system possesses good thermal stability and suitable fragility, hence they can be classified with strong glass series. Subsequently, we prepared Er^{3+} -doped zinc tellurite glass containing silver NPs and the improvement in their optical properties were reported [3, 11-13]. However, to the best of our knowledge, there is no report on the effect of silver NPs on thermal stability, fragility and chemical durability of tellurite glasses while the embedment of metallic NPs was routinely done in recent years. It is of paramount importance to study the thermal and chemical durability of such materials prior to the fabrication of devices. Therefore, the aim of present paper is to investigate the thermal stability, fragility and chemical durability of Er^{3+} -doped zinc tellurite glass with and without silver NPs in different solutions. A series of glasses are prepared by melt quenching method and their surface morphology, chemical and thermal properties are characterized in detail. The results are analyzed and different mechanisms are proposed.

2. Experimental procedures

A series of glass samples of composition $(79-y)\text{TeO}_2-20\text{ZnO}-1\text{Er}_2\text{O}_3-y\text{AgCl}$ ($y=0, 0.5, 1, 2$ and 3 mol%) were prepared by melt quenching method and labeled as S1, S2, S3, S4, and S5 respectively. The well-mixed powder of starting materials with high purity was melted at $800\text{ }^\circ\text{C}$ inside a porcelain crucible using a rising heart electronic furnace (Carbolite ELF 11/6B). After 20 minutes, the completely viscous melt were quenched between two stainless steel moulds preheated at $300\text{ }^\circ\text{C}$ and kept inside the annealing furnace for 3 hours before cooling down slowly to room temperature. The transparent samples were grained by different sand papers from 100 to 1200 and polished carefully using diamond paste and W Lubricant Hyprez Diamond Compound liquid. The square-shaped samples were finally cut to achieve $20\times 20\times 2.7$ mm sample size.

In order to examine the chemical durability of tellurite glass samples, 4 pieces of each sample were prepared. The sample pieces were weighted using analytical digital balance (AND, GR-200) by error in the order of $\pm 10^{-4}$ gm. One sample was kept as a reference (R), and the other three pieces were put in 5 mL of different de-ionized water (labeled as W), hydrofluoric acid (Orec, 49% labeled as F) and ammonium hydroxide (Mallinckrodt Chemicals, 30% NH_4OH , labeled as N). These series of samples series are designated as S_xR , S_xW , S_xF and S_xN , respectively, corresponding to $x=1, 3, 4$ and 5 labeled the samples as S1, S3, S4 and S5, respectively. However, the chemical durability of the sample S2 was not examined. The samples were kept in different solutions for 4, 9 and 21 days. After each time interval, the samples were washed by running water, and dried at $127\text{ }^\circ\text{C}$ for 15 min in furnace and weighted by the same balance. The mass loss (W_L) was calculated using,

$$W_L = \frac{W_B - W_A}{W_A} \times 100 \quad (1)$$

where W_A and W_B refer to sample weights after and before corrosions respectively.

Atomic force microscope (AFM, SPI3800 built by Seiko Instrument Inc. (SII)) was used to observe the morphological change of the surface of glasses before and after corrosions. Furthermore, the morphology and elemental analysis of the glass surface were investigated by recording the energy dispersive X-ray (EDX) spectra using a SwiftED3000 EDX attached to a TM3000 Hitachi tabletop scanning electron microscope (SEM). Thermal characteristics of samples were obtained using a differential thermal analyzer (DTA, Model: Pyris Diamond TG-DTA, Japan) by heating at a rate of $10\text{ }^\circ\text{C}/\text{min}$ in the temperature range $260-650\text{ }^\circ\text{C}$ to determine the endothermic and exothermic peaks. The glass onset transition temperature (T_g) was estimated using the average temperature between beginning of transformation and minimum point. The glass onset crystallization temperature was determined considering the starting temperature of

crystallization, T_x . The stability of glass was evaluated by measuring the difference between defined glass transition and crystallization temperatures [14].

$$\Delta T = T_x - T_g \quad (2)$$

Fragility of glasses was also investigated by measuring the glass transition width. Optical and structural properties of prepared Er^{3+} -doped zinc tellurite glass containing silver NPs is reported elsewhere [15].

3. Results and discussion

Fig.1a shows typical view of sample S1 during the process of polishing by 1200 sand paper. Fig.1b presents the reaction of HF by different samples at very beginning moment of immersion. Pouring the HF into the bottles containing the S2 to S5 samples (marked as S2F to S5F) resulted in a violet layer around the sample, which disappeared gradually in few hours. These samples started to destruct and dissolve in HF, very rapidly so that in only 4 days they became in a very muggy powder form and were inappropriate to measure their weights (Fig.1c). The S1R sample not reacted swiftly, however it began to weather and was consequently broken to two pieces after one day. The SxW sample series remained almost unchanged in color and surface morphology as observed by unarmaged eye, after few days (Fig.1d). The surface of SxN series were almost rusted after one day, however, the damage was not as substantial as SxF series. After four days corrosion in NH_4OH , the samples became completely covered by a white layer and lost their transparency (Fig.1d). Our observation showed that the thickness of this layer decreases with increasing the concentration of Ag NPs in tellurite samples. Therefore, silver NPs played an important influence on the chemical durability of the tellurite glass.

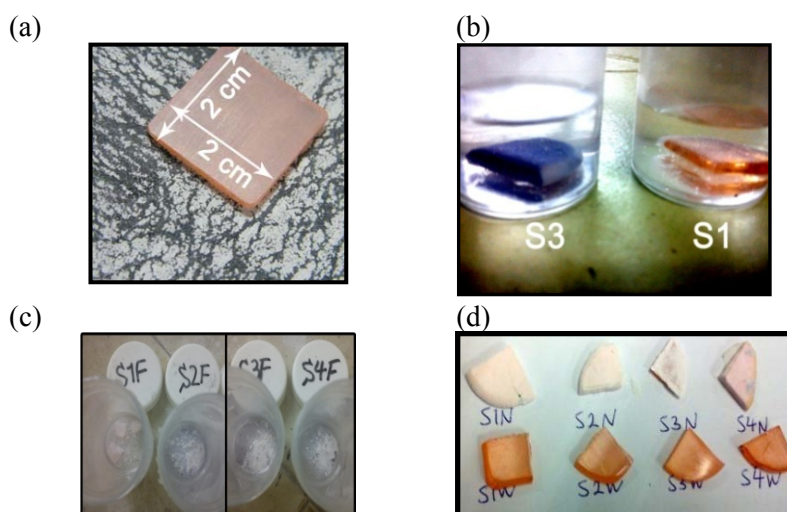
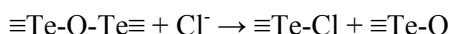


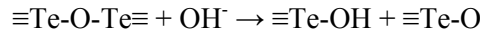
Fig.1. Graining of sample S1 (a). Attack by HF on S1 and S3 tellurite glasses immediately after replacing in solution (b). Samples in HF transformed to wet powders after corrosion for 4 days (c). Loss of transparency of samples kept in NH_4OH and water after 4 days (d).

It is well known that the tellurium dioxide (TeO_2) is a poor glass former. However, addition of only a little alkali or other modifiers is enough to form a glass by a fast melt quench technique. One of the important properties of tellurite glass is their high solubility of rare earth with respect to silicate and phosphate glasses [16]. It is due to weaker 2-dimensional Te-O bond in compare to strong covalent Si-O and P-O linkages. On the other hand, ionic diameter of Te is larger than Si, which results in weaker network and facilitates the incorporation of any modifier and dopant. Therefore, the tellurite glass network can be easily attacked by alkali, halide or acidic solutions. Addition of AgCl leads to modification of tellurite network by halide ions as

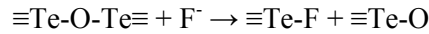


The bond energy of $\equiv\text{Te-Cl}$ or $\equiv\text{Te-O}$ is proportional to the charge density of anion (z/a^2). The charge density of O^{2-} and Cl^- are 102.04 and 30.52 nm^{-2} respectively [17]. Addition of AgCl decreases the number of Te-O linkages, therefore, the average tellurite bond energy reduces which results in the formation of more attackable network.

The Te-O-Te network is attacked and broken by OH^- ions through a nucleophilic attack as



and



for tellurite glass in HF solution. Depolymerization of tellurite glass by F^- ions is faster and stronger than OH^- ions due to larger electronegativity of F^- than O^{2-} ions. The samples containing silver NPs show lower chemical durability in HF solutions as they are leached in few seconds and became powder in less than 4 days. This can be attributed to the decrease in oxygen packing density in S3, S4 and S5 samples compared to S1 tellurite glass sample.

Fig.2a shows the weight loss of S1, S3, S4 and S5 samples in de-ionized water. By and large, the water resistivity of samples is decreased by addition of AgCl up to 1 mol%, while it is improved for 2 and 3 mol% AgCl contents. The weight loss of samples in NH_4OH solution is shown in Fig.2b. In particular, the introduction of AgCl up to 2 mol% decreased the chemical durability of tellurite glass samples, while it is developed by 3 mol% AgCl . The weight of SxN samples increases after four days due to deposition of dissolved components on the surface of samples. It can be concluded that the corrosion was stopped between the fourth and ninth day. Therefore, the solved component in saturated solution started to deposit on the surface and edges of samples which resulted in granulated clusters and increased the weight of samples. After nine days, however, the transparency of samples containing silver NPs (SxN) was higher than sample without Ag NPs, where some parts of surface remains with no deposited layers.

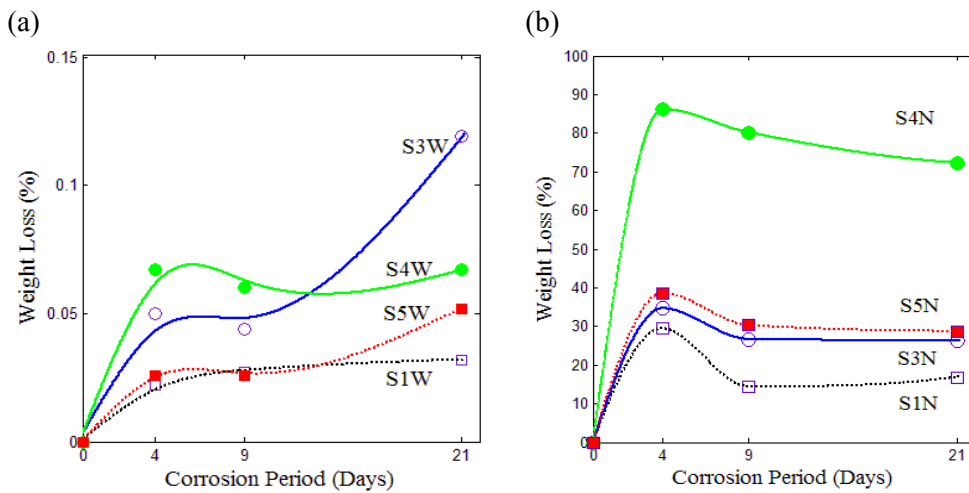


Fig.2. Weight loss of different tellurite glass samples in water (a) and NH_4OH (b).

Fig.3a to 3f depict the topography of the samples S1 and S3 before (a and d), and after replacing in water for 4 days (b and e) and 21 days (c and f) respectively. Comparing with the as-polished surfaces (a and d), the surface of samples under corrosion by water are more rough. The surface of samples (S2W) after 21 days shows complete lopsided feature. The root mean square (RMS, δ) of the surface roughness of each glass is also indicated in the Fig.3, collected by software analysis (NavoNavi Station version 5.01C). The moderated RMS of sample S1 (Fig.3.a-c) signifies the quasi-steady state condition of weight of the sample S1W after a period of 4 days up to 21 days. The increased RMS values of sample S3W is consistent with large change in the surface morphology after 21 days (Fig.3f).

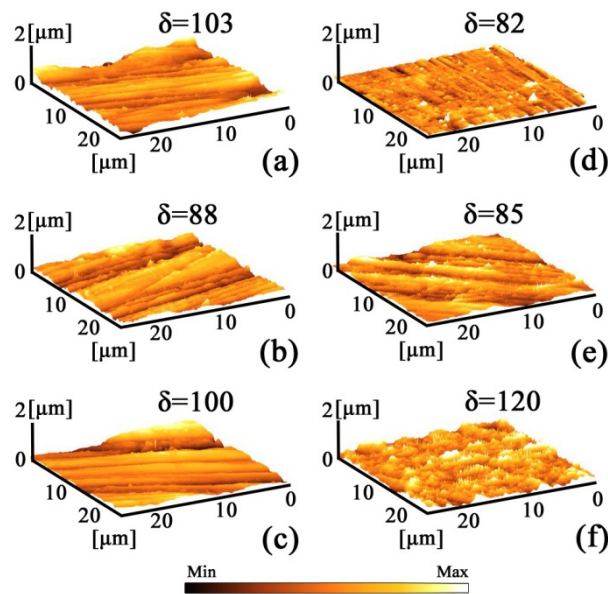


Fig.3. The AFM micrograph of *S1R* (a) and *S1W* for 4 days (b) and 21 days (c), while (d), (e) and (f) corresponds to their counterpart samples containing 1 mol% AgCl (*S3*). Corresponding root mean square (RMS) surface roughness of each sample is denoted as δ .

Fig.4a shows the SEM micrograph of sample *S1*. There are only parallel lines observed which originated from the polishing process. Fig.4b shows the surface morphology of sample *S1N* after replacement in NH_4OH solution for 21 days. The surface can be divided into two distinct regions; the rich-tellurium area (Fig.4c) and the rich-zinc and oxygen area (Fig.4d). Fig.5 presents the morphology of samples *S3* (a) and *S2N* (b) after corrosion by NH_4OH solution for 21 days. Two distinct regions marked as 1 and 2 are also observed in Fig.5b. The first region (Fig.5.c) is enriched by silver. The percentage of each cation is decreased in second region (Fig.5.d) while oxygen contribution is increased that is likely due to enlarged metal-OH bonds density. The calculated and experimental weight percent participation of each element in different areas of Fig.4b and Fig.5b are listed in Table 1.

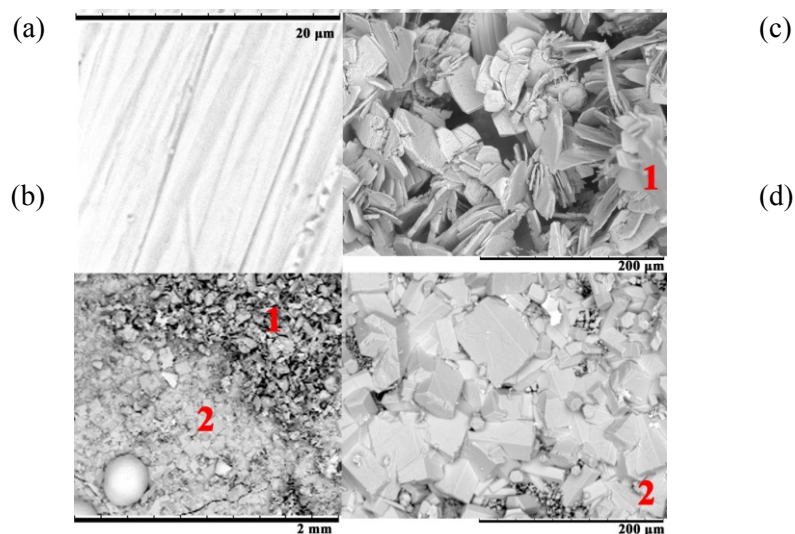


Fig.4 SEM of glass *S1* (a) and *S1N* after 21 days (b). The insets (c) and (d) shows the regions defined in (b). The corresponding EDX analysis for region 1 and 2 are given below.

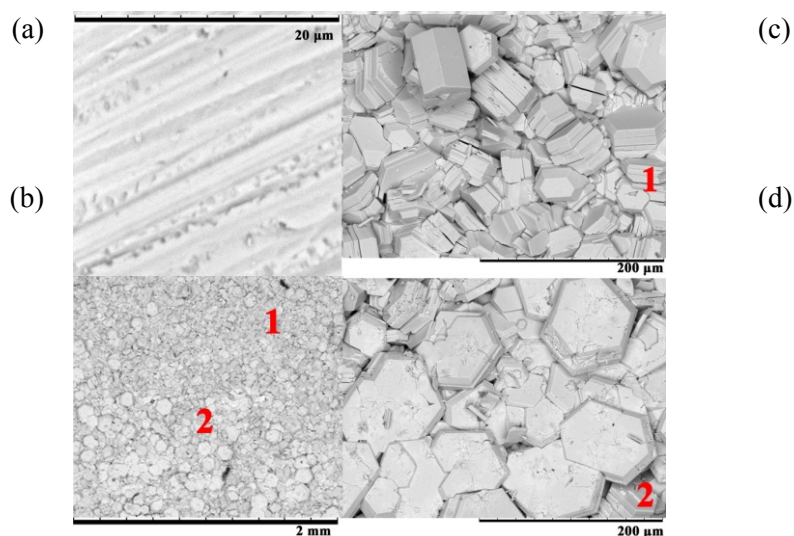


Fig.5 SEM of glass S3 (a) and S2N after 21 days (b). The insets (c) and (d) shows the regions defined in (b). The corresponding EDX analysis for region 1 and 2 are given below.

The analysis of EDX spectra are shown in Fig. 6 and used to evaluate the amount of each element on the surface of glasses. The relative weight percentage of each element on the surface of S1N and S3N glass samples are summarized in Table 1. As mentioned above, in some regions of the weathered samples the existence of tellurium is very high, while in some areas its abundance is relatively lower. This may be attributed to the dissolution of tellurium in the solution, clustering and deposition on the surface of the glass. As a result of these mechanisms, the change in weight loss is miniature, however, the surface morphological element distribution is extensive.

Table 1. Calculated and experimental weight of the elements on the surface of as-prepared and weathered glasses.

Sample		O (%)	Zn (%)	Te (%)	Er (%)	Ag (%)	Cl (%)
S1	Calculated	19.81	8.94	68.96	2.29	-	-
S1	Experimental	19.810	10.118	66.027	4.045	-	-
S1N-21d	Region1	13.153	1.010	85.837	0.000	-	-
S1N-21d	Region2	27.831	22.139	49.575	0.455	-	-
S3	Calculated	19.61	8.96	68.16	2.29	0.74	0.24
S3	Experimental						
S3N-21d	Region1	11.478	0.250	84.156	0.267	3.756	0.093
S3N-21d	Region2	16.422	0.213	81.561	0.055	1.703	0.045

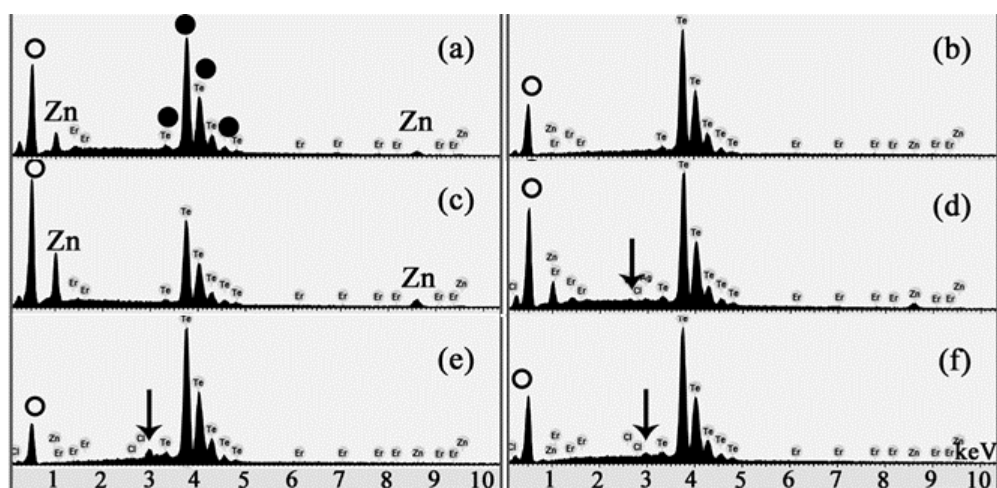


Fig.6. EDX spectra of samples S1 and S3 for zero (a, d) and 21 (b, c, e, f) days weathering in NH_4OH solution. Insets (b, c) and (e, f) correspond to regions 1 and 2 as depicted in Fig.4 and Fig.5, respectively. The peaks of oxygen (O), Te (●), Zn and Ag (↓) are highlighted in the rich areas.

Fig.7a shows the DTA curves of as-polished samples (before exposing in any solution). The glass transition temperature, T_g , the onset crystallization temperature, T_x , the crystallization peak, T_p , and the melting point, T_m , of the sample S1 are labeled in Fig.6a and are listed in Table 2. Introduction of Ag NPs results a decrease in the glass transition temperature, which is due to the increased disorder by NPs while the number of linkages decrease slightly. The onset crystallization temperature of Er^{3+} -doped zinc tellurite glass initially increases by addition of AgCl up to 1 mol%. However, further addition of AgCl leads to a decrease in the onset crystallization temperature. Two crystallization peaks, T_p , in Er^{3+} -doped zinc tellurite glass were observed which shifted toward lower temperatures by the addition of Ag NPs. It is interesting to note that the incorporation of NPs replaces the prominent crystallization peak by a smaller crystallization peak. The first crystallization peak in this system can be attributed to TeO_2 and ZnTeO_3 and the second peak is assigned to ZnTe_3O_8 crystalline phases [18]. The suppression of the first exothermic crystallization peak is attributed to change in the environment which slows the rate of crystallization process [19]. The stability of the glasses is estimated by taking the difference between onset crystallization temperature and glass transition temperature into account. As shown in inset of Fig.7b, the glass thermal stability is maximized for S2 glass sample and is decreased by further increase of molar percentage of Ag NPs.

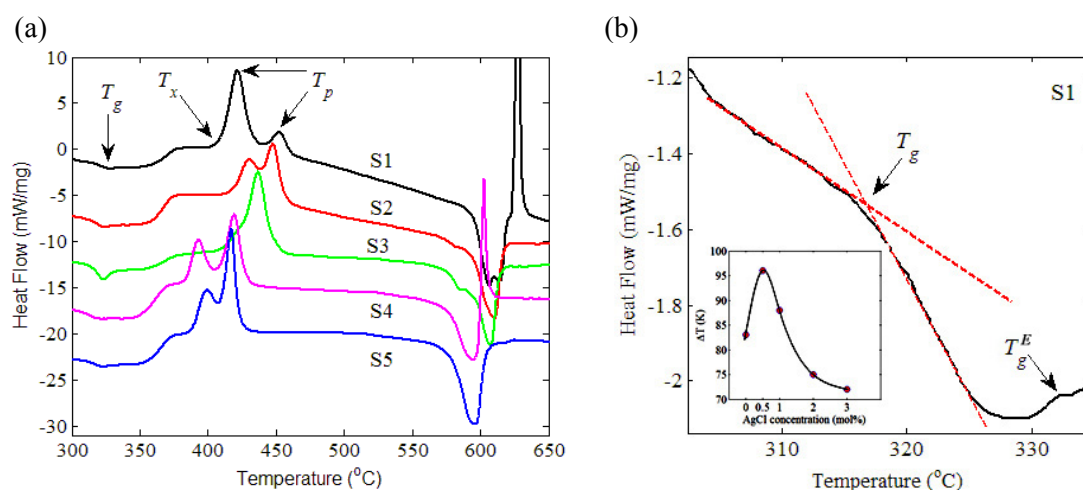


Fig.7. DTA curves of Er^{3+} -doped zinc tellurite glass with different concentration of Ag NPs (a) and determination of the glass transition temperature (b). Inset of (b) shows the variation of the AgCl concentration dependent thermal stability.

Fragility of the glasses can be evaluated from the glass transition width ΔT_g , which can be determined as the gap between onset glass transition temperature (T_g) and temperature (T_g^E) at which the transition is completed ($\Delta T_g = T_g^E - T_g$). The larger ΔT_g corresponds to the stronger glass former [20, 21]. Determination of glass transition widths of sample S1 is illustrated in Fig.7b, and its value for all glasses is listed in Table 1. It is found that the addition of silver NPs into the erbium-doped zinc tellurite glass strengthen the glass structure and thereby reduces the fragility. However, for sample doped with 3mol% AgCl (the maximum concentration) a small reduction in ΔT_g ($\sim 1^\circ\text{C}$) is observed. The glass strength is approved about 20, 29, 40 and 38 percent by addition of 0.5, 1, 2 and 3 mol% AgCl, respectively.

Table 2. Thermal properties of Er^{3+} -doped zinc tellurite glasses containing Ag NPs.

Glass Label	Composition (mol%)	T_g	T_x	T_p^1	T_p^2	T_m	ΔT	T_g^E	ΔT_g
S1	79TeO ₂ -20ZnO-1Er ₂ O ₃	317	400	421	452	607	83	317	15
S2	78.5TeO ₂ -20ZnO-1Er ₂ O ₃ -0.5AgCl	312	408	430	447	610	96	330	18
S3	78TeO ₂ -20ZnO-1Er ₂ O ₃ -1AgCl	314	402	436	-	607	88	335	21
S4	77TeO ₂ -20ZnO-1Er ₂ O ₃ -2AgCl	303	378	392	419	594	75	328	25
S5	76TeO ₂ -20ZnO-1Er ₂ O ₃ -3AgCl	309	381	399	417	595	72	333	24

The incorporation of AgCl into (79-x)TeO₂-20ZnO-1Er₂O₃-xAgCl glass system decreases the oxygen packing density (OPD). Therefore, the compactness of the glass decreases. Taking into account, the molar volume and coordination number of glass series, one can see that the bond density in the proposed samples decrease by increasing the AgCl content. Reduction in the glass transition temperature and chemical durability of glasses after the addition of AgCl are due to structural changes in the glass samples so that the glass losses the compactness and average bonds strength. Conversely, it is shown in paper that the thermal stability and the strength of the glass in the region of glass transition temperature is enhanced due to the addition of AgCl up to 1 and 2 mol%, respectively.

4. Conclusion

Chemical resistivity, thermal stability and fragility of the prepared Er^{3+} -doped zinc tellurite glasses containing silver NPs are examined by means of weight loss in different solutions, AFM, SEM, EDX, and DTA techniques. The incorporation of silver NPs reduces the chemical stability and water resistivity of glasses as shown by weight loss measurements. The weathering of samples is explained by OH group attacks. The increase in the attack and thereby the weight loss for samples containing silver NPs are attributed to the decrease in average bond energy of glasses. In contrast, the introduction of silver NPs increases the thermal stability, and modified the fragility of glasses as evidenced from DTA data analysis. The onset glass transition temperature and the crystallization temperature of the glasses are found to decrease with the increase in the silver content. It is worth to look at the photoluminescence, absorption and Raman spectra of these samples for further insight. The proposed glasses showed improved thermal stability which make them suitable candidate for fiber drawing. The influence of metallic NPs on chemical and thermal durability of rare-earth doped glasses is of imperative effects to determine their capabilities for device fabrication.

Acknowledgements

The financial supports from Ministry of Higher Education (GUP, Malaysia) through the research grant (Vote 04L32) and UTM.J.10.01/13.14/1/128/IDF are gratefully acknowledged. Dr. M. Reza Dousti would like to thank Iran Nanotechnology Council for ongoing incentives.

References

- [1] R.de Almeida, D.M.da Silva, L.R.P. Kassab, C.B.de Araujo, *Opt. Commun.* **281**, 108 (2008)
- [2] S.P.A. Osorio, V.A.G. Rivera, L.A.O. Nunes, E. Marega Jr., D. Manzani, Y. Messaddeq, *Plasmonics* **7**, 53 (2012).
- [3] M. Reza Dousti, M.R. Sahar, S.K. Ghoshal, Raja J. Amjad, R. Arifin, *J. Non-Cryst. Solids* **358**, 2939 (2012)
- [4] V.A.G. Rivera, Y. Ledemi, S.P.A. Osorio, D. Manzani, Y. Messaddeq, L.A.O. Nunes, E. Marega Jr., *J. Non-Cryst. Solids* **358**, 399 (2012).
- [5] P.R. Watekar, S. Ju, W.T. Han, *Colloid. Surface. A* **313–314**, 492 (2008).
- [6] H.V. Walters, P.B. Adams, *Appl. Opt.* **7**(5), 845 (1968).
- [7] E. Stavrou, S. Kriptou, C. Raptis, S. Turrell, K. Syassen, *Phys. Status Solidi C.* **8**, 3039 (2011).
- [8] M.R. Sahar, K. Sulhadi, M.S. Rohani, *J. Non-Cryst. Solids* **354**, 1179 (2008).
- [9] E.A. Mohamed, F. Ahmad, K.A. Aly, *J. alloys. Compnd.* **538**, 230 (2012).
- [10] H.A.A. Sidek, S. Rosmawati, Z.A. Talib, M.K. Halimah, W.M. Daud, *American J. Appl. Sci.* **6**, 1489 (2009).
- [11] M. Reza Dousti, M.R. Sahar, S.K. Ghoshal, Raja J. Amjad, R. Arifin, *J. Mol. Struct.* **1033**, 79 (2013).
- [12] S.K. Ghoshal, A. Awang, M.R. Sahar, R.J. Amjad, M.R. Dousti, *Chalcogenide Letters*, **10**(10), 411 (2013).
- [13] M.R. Dousti, M.R. Sahar, R.J. Amjad, S.K. Ghoshal, A. Awang, *J. Lumin.* **143**, 368 (2013).
- [14] S. Mahadevan, A. Giridhar, A.K. Singh, *J. Non-Cryst. Solids* **88**, 11 (1986).
- [15] M. R. Dousti, M.R. Sahar, S.K. Ghoshal, R. J. Amjad, A.R. Samavati, *J. Mol. Struct.* **1035**, 6 (2013).
- [16] R.A.H El-Mallawany, *Tellurite Glasses Handbook: Physical Properties and Data*, CRC Press, (2002).
- [17] H.S. Liyan, Z. Chunlei, Y. Zhongchao, D.J. Zhang, S. DaiaLili, Hu and Z. Jiang, *Solid State Commun.* **134**, 449 (2005).
- [18] A. Nukui, T. Taniguchi, M. Miyata, *J. Non-Cryst. Solids.* **293–295**, 255 (2001).
- [19] S. Banijamali, B. Eftekhari Yekta, A.R. Aghaei, *J. Non-Cryst. Solids.* **358**, 303 (2012).
- [20] T. Moynihan, *J. Am. Ceram. Soc.* **76**, 1081 (1993).
- [21] D. Zhu, C. S. Ray, W. Zhou, and D. E. Day, *J. Non-Cryst. Solids* **319**, 247 (2003).